Sum Frequency Generation and Catalytic Reaction Studies of the Removal of Organic Capping Agents from Pt Nanoparticles by UV−Ozone Treatment

Cesar Aliaga, Jeong Y. Park, Yusuke Yamada,† Hyun Sook Lee, Chia-Kuang Tsung, Peidong Yang, and Gabor A. Somorjai*

Department of Chemistry, University of California, Berkeley, California 94720, and Materials Sciences Division and Chemical Sciences Division, Lawrence Berkeley National Laboratory, Berkeley, California 94720

Received: December 10, 2008; Revised Manuscript Received: January 22, 2009

We report the structure of the organic capping layers of platinum colloid nanoparticles and their removal by UV−ozone exposure. Sum frequency generation vibrational spectroscopy (SFGVS) studies identify the carbon−hydrogen stretching modes on poly(vinylpyrrolidone) (PVP) and tetradecyl tributylammonium bromide (TTAB)-capped platinum nanoparticles. We found that the UV−ozone treatment technique effectively removes the capping layer on the basis of several analytical measurements including SFGVS, X-ray photoelectron spectroscopy, and diffuse reflectance infrared Fourier transform spectroscopy (DRIFTS). The overall shape of the nanoparticles was preserved after the removal of capping layers, as confirmed by transmission electron microscopy (TEM). SFGVS of ethylene hydrogenation on the clean platinum nanoparticles demonstrates the existence of ethylidyne and di-σ-bonded species, indicating the similarity between single-crystal and nanoparticle systems.

I. Introduction

Industrial heterogeneous catalysts are usually composed of nanometer-sized metallic clusters capped with diverse organic compounds and supported by porous materials. Traditionally, fundamental catalysis studies are conducted on metal single crystals, which provide extensive information of the molecular processes at the surface under optimal, well-controlled conditions. However, most of the industrial catalysts are highly dispersed nanoparticles, and catalytic processes occur at elevated temperatures and high pressures.[1,2] Therefore, it is essential to perform *in situ* studies of model systems that have complexities associated with real catalytic conditions.[3] The evolution of the science of nanomaterials has permitted the use of nanoparticles as model systems,[4] and the capability of controlling their size, shape, and composition by colloid chemistry brings about new opportunities to develop novel nanocatalysts.[5,6]

Colloidal nanoparticle synthesis involves the reduction of metal ions in solution, and because the surface energy of finely divided matter is high, freshly precipitated metallic particles naturally tend to aggregate. To overcome this problem, freshly prepared nanoparticles are usually precipitated in a solution that contains an organic compound that will adhere to their surface and keep the particles suspended.[7] After transfer to a solid support, this capping layer remains at the surface of the particles. It is known, however, that on the molecular scale the organic capping layer contains open spaces that permit the reactant and product molecules to adsorb and desorb from the surface of the catalytically active metal. Earlier studies have indicated that catalytic activity greatly depends on the nature of the interaction between the molecules and the metal sites.[8,9] However, the role of the capping agent in the catalytic activity and selectivity is poorly understood in spite of its importance in heterogeneous catalysis as an emerging model system.

Sum frequency generation vibrational spectroscopy (SFGVS) is an important tool in the basic understanding of catalysis on the molecular level because it is able to identify reaction intermediates under catalytic conditions. Several SFGVS studies on catalytic reactions, including CO oxidation over colloid nanoparticles, were carried out earlier. The vibrational signature of CO does not overlap with the capping agent vibrational modes, facilitating the interpretation of the resulting spectra.[10−12] Other reactions, such as pyridine hydrogenation, were also investigated, although only outside of the methyl−methylene stretch vibrational region.[13] Reactions more relevant to the industrial processes of hydrogenation and cracking have been performed on platinum single crystals and probed by SFGVS but have not been carried out on nanoparticles because of the aforementioned difficulty.[14,15]

The approach to investigating the role of capping agents involves the removal of capping layers with UV−ozone (O_3) treatment. UV−ozone oxidation has been used for decades as a means of cleaning slightly soiled surfaces for a variety of applications. The method typically uses ultraviolet light that includes wavelengths of 185 and 257 nm, where the former generates ozone upon interacting with molecular oxygen. The UV−ozone oxidation process involves the simultaneous action of ozone and ultraviolet light, which are responsible for the oxidation of the carbon-containing compounds into carbon dioxide and water.[16] Ultraviolet radiation can also be used for polymer surface modification with applications in photolithography, microfluidics, and bioengineering, and its surface effects were studied using SFGVS,[17,18] which was also used to investigate the effect of ultraviolet radiation and ozone on typical organic substances present in the upper atmosphere.[19] Earlier results of removal of the capping agent using the same method were furthermore reported for gold nanospheres with satisfactory results as well as for bimetallic PtFe nanoparticles.[20,21]

* Author to whom correspondence should be addressed. E-mail: somorjai@berkeley.edu.

† Current address: Research Institute of Ubiquitous Energy Devices, National Institute of Advanced Industrial Science and Technology (AIST), 1-8-31 Midorigaoka, Ikeda, Osaka 563-8577 Japan.

10.1021/jp8108946 CCC: $40.75
Published on Web 02/20/2009

In this work, the application of UV−ozone oxidation is used to remove the capping agent so that SFGVS catalysis studies at the surfaces of nanoparticle catalysts can be carried out. Previous attempts using methods such as plasma cleaning, hydrogen treatment, or heat treatment under different gaseous atmospheres proved to be inefficient because of the irreversible modification of the shape and distribution of the nanoparticles. We monitored the removal of the capping agent from the surface of platinum nanocubes with various analytical methods including SFGVS, XPS, and DRIFTS. The shape and spatial distribution of the nanoparticles are examined with SEM and TEM before and after UV−ozone treatment. In addition, ethylene hydrogenation at room temperature and atmospheric pressure is performed at the surface of the catalytic nanocubes, and the reaction intermediates are probed with SFGVS.

II. Experimental Procedures

II.a. Synthesis of TTAB- or PVP-Capped Nanoparticles. The nanoparticles used in this study consist of 10 nm platinum cubes capped with tetradecyl trimethylammonium bromide (TTAB) or polivynil pyrrolidone (PVP). TTAB-coated platinum nanocubes were synthesized according to literature methods.[6] Aqueous solutions of tetradecyltrimethylammonium bromide (400 mM, 2.5 mL) and dipotassium tetrachloroplatinate(II) (10 mM, 1 mL) were added to water (5.9 mL) in a reaction vial at room temperature. The solution was mixed with a vortex mixer for 30 s and was allowed to stand until needle-shaped crystals formed. The mixture was then heated to 50 °C in an oil bath under magnetic stirring until the crystals dissolved. An ice-cooled aqueous solution of sodium borohydride (500 mM, 0.6 mL) was added rapidly to the solution. The hydrogen gas formed was released via a needle through the rubber septum capping the reaction vial. The needle was removed after 15 min of reaction. The reaction mixture was then magnetically stirred for more than 7 h at 50 °C. The resulting brown solution was centrifuged at 3000 rpm for 30 min to remove the larger Pt nanoparticles. The supernatant solution was separated and centrifuged again at 12 000 rpm for 10 min. The precipitate was collected and redispersed in deionized water.

The synthesis of PVP-capped Pt nanoparticles is described elsewhere.[22] Briefly, 0.1 mmol of ammonium hexachloroplatinate(IV), 1.5 mmol of trimethyl(tetradecyl)ammonium bromide, and 2 mmol of poly(vinylpyrrolidone) were added to 20 mL of ethylene glycol in a 50 mL three-necked flask at room temperature. The stock solution was heated to 80 °C in a Glas-Col electromantle (60 W, 50 mL) with a Cole-Parmer temperature controller (Diqi-sense) and was evacuated at this temperature for 20 min to remove water and oxygen under magnetic stirring. The flask was then heated to 180 at 10 °C/min and was maintained at this temperature for 1 h under Ar. When the reaction was complete, excess acetone was added at room temperature to form a cloudy black suspension. This suspension was separated by centrifugation at 4200 rpm for 10 min, and the black product was collected by discarding the colorless supernatant. The precipitated platinum nanocrystals were washed twice by precipitation/dissolution (redispersed in 7.5 mL of ethanol with sonication and then precipitated by adding 37.5 mL of hexanes).

II.b. Analytical Methods. The shape and size distribution of the particles, deposited on a standard silica grid, were monitored with a TEM FEI Tecnai 12 operating at 100 kV. For spectroscopic purposes and XPS measurements, the nanoparticles were deposited either by drop casting or by using the Langmuir−Blodgett (LB) technique.[22] The nanoparticle surface monolayer was compressed at a rate of 20 cm^2/min, and the deposition of the nanoparticles was carried out by lifting the substrate that was previously submerged in water. The change in morphology of the 2D array of PVP-coated nanoparticles was characterized with SEM before and after the removal of the polymer capping agent. A Zeiss Gemini Ultra-55 analytical scanning electron microscope was used for this study.

The irradiation of the nanoparticles was conducted *ex situ* using a Bulbtronics 16 W low-pressure mercury lamp emitting at 185 and 257 nm inside a custom-made metallic enclosure. The sample was positioned 5 mm from the ultraviolet lamp's quartz tube surface for a determined amount of time and then removed from the UV chamber. The films used for SFG measurements were deposited on the surface of silica prisms that were irradiated and subsequently attached to a custom-made SFG reaction cell for in situ spectroscopy in nearly total internal reflection (TIR) geometry, pressed against a Kalrez O-ring by a Teflon block with two set screws. For catalytic studies, a mixture of 35 Torr of ethylene (Matheson 99.98%), 150 Torr of hydrogen (ultrahigh purity Matheson), and argon (ultrahigh purity Matheson balanced to 760 Torr) was introduced into the cell, which is connected to a gas manifold through stainless steel tubing. The mixture was circulated using a recirculation pump (Metal Bellows Div.) in order to maintain a homogeneous concentration and temperature of reactants and products in the reactor volume.

The SFG spectrometer consists of a mode-locked Continuum Nd:YAG laser emitting at 1064 nm with a pulse width of 20 ps and a 20 Hz repetition rate. It generates pulsed beams of tunable IR (2750−3600 cm^{-1}) and 532 nm light at angles of 60 and 55°, respectively, with respect to the sample surface normal. The beam energies are 100 and 80 μJ for the tunable IR and 532 nm beams, respectively, and they are considerably defocused in order to decrease the energy density due to the size and weak bonding of the nanoparticles to the support because previous studies have demonstrated that higher energies could remove them from the surface.[10] The infrared, 532 nm, and sum frequency beams are p-polarized. The sum frequency signal is passed through a monochromator and collected by a photomultiplier tube. The resulting signal is sent to a gated integrator, and the sum frequency output is normalized by the intensity of the infrared beam.

SFG is second-order nonlinear spectroscopy and is sensitive to molecules in noncentrosymmetric environments. Even though nanoparticle systems are inherently centrosymmetric, the TIR geometry circumvents this problem because of the evanescent nature of the electric fields as the distance from the prism surface increases.[23,24] The second-order nonlinear polarization $\mathbf{P}^{(2)}_{(\omega 1+\omega 2)}$ is described by

$$P^{(2)} = \chi^{(2)}{:}E(\omega_{vis})\,E(\omega_{IR}) \tag{1}$$

where $\mathbf{E}(\omega_i)$ is the electric field of the incoming beam and $\chi^{(2)}$ is the second-order nonlinear susceptibility. The susceptibility has a nonresonant contribution $\chi^{(2)}_{NR}$ and a resonant contribution $\Sigma\chi^{(2)}_R$. $\chi^{(2)}_{NR}$ is a background contribution from the interface, and $\Sigma\chi^{(2)}_R$ includes contributions from individual resonance modes $\chi^{(2)}_R$. The expression for $\chi^{(2)}_R$ is

$$\chi^{(2)}_R = \left(\frac{N\langle\beta^{(2)}\rangle}{\omega_{IR} - \omega_q + i\Gamma_q}\right) \tag{2}$$

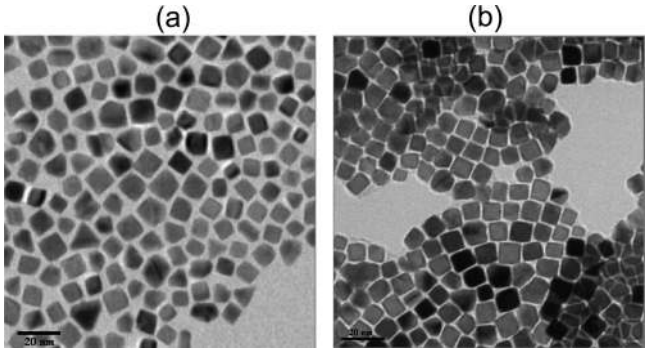

Figure 1. TEM images of a Langmuir−Blodgett film of 10 nm platinum cubes (a) before and (b) after 2 h of UV−ozone treatment.

where N is the number of modes contributing to the SFG signal, Γ_q is the damping constant for the qth vibrational mode with a frequency of ω_q, ω_{IR} is the frequency of the incoming IR beam, and $\beta^{(2)}$ is the molecular hyperpolarizability averaged over all possible molecular orientations and contains the Raman polarizability and the IR transition dipole moment. The intensity of the SFG signal is proportional to the square of the absolute value of the nonlinear polarization.[25−27]

III. Results and Discussion

III.a. TEM and SEM Characterization of the Morphological Change of Pt Nanoparticles after UV−Ozone Treatment. Transmission electron microscopy (TEM) was performed on TTAB- and PVP (not shown)-coated platinum nanocubes deposited on a carbon grid in order to characterize the surface before and after the treatment to observe whether any changes in shape or aggregation occur. Figure 1a,b shows TEM images of the freshly prepared TTAB-coated Pt cubes and after 2 h of UV−ozone treatment, respectively. The distance between particles slightly decreases from an average of 2.5 nm to an average of 0.9 nm, suggesting a substantial reduction of the amount of capping agent, and the shape and size of the particles are conserved. This is in contrast to the method of oxygen plasma treatment traditionally used to oxidize organic molecules adsorbed on surfaces, which in the case of platinum nanoparticles results in the fusion of the particles, thus irreversibly modifying both the shape and distribution.

SEM was performed on films of PVP- and TTAB (not shown)-coated platinum nanocubes deposited on silicon wafers. Figure 2a,b shows SEM images of a 2D array of PVP-coated nanocubes taken before and after 270 min of irradiation with UV−ozone. The SEM image reveals individual nanoparticles that are 12 nm in size and indicates that the nanoparticles do not agglomerate upon UV−ozone treatment.

III.b. X-ray Photoelectron Spectroscopy (XPS) Characterization of PVP- and TTAB-Coated Platinum Nanocubes before and after UV−Ozone Treatment. The XPS experiments were conducted on nanoparticle films deposited on silicon wafers. Spectra were taken before and after UV−ozone treatment. Figure 3a,b shows the XPS results for TTAB- and PVP-coated platinum nanocubes, respectively. In Figure 3a, the ratio of Pt 4f/C 1s increases 4.4 times after 2 h of UV−O_3 treatment. It was not possible to detect nitrogen with XPS for these particles because of the small amount of nitrogen in the TTAB molecule. The changes in the platinum peaks also show that the nanoparticles partially oxidize after the treatment. Figure 3b shows the XPS results for the PVP-coated nanoparticles. The considerably higher amount of nitrogen in the PVP molecule allows for a detailed analysis of the evolution of the nitrogen 1s peak. The Pt 4f/N 1s ratio changes from 0.97 for the fresh sample to 0.055 after 270 min of irradiation, suggesting the effective removal of the capping agent. As in the previous case, an oxidation of the platinum metal takes place.

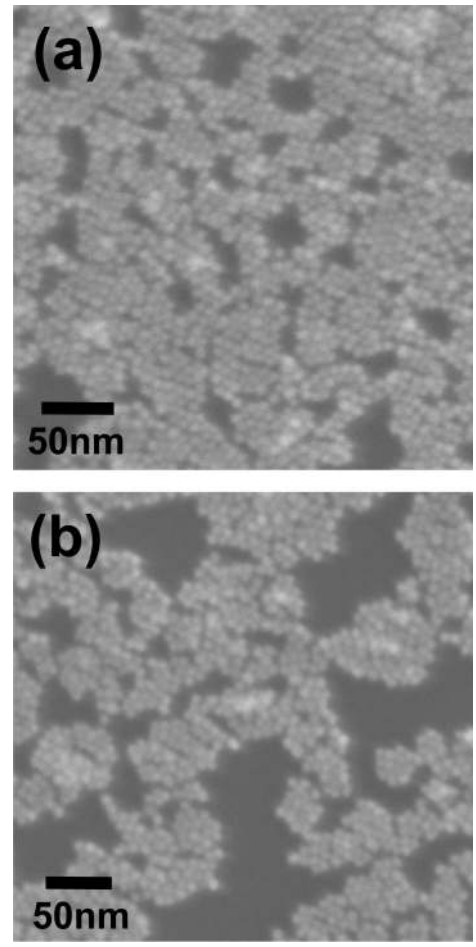

Figure 2. (a) SEM images of PVP-coated nanoparticles on a silicon wafer (a) before and (b) after UV−ozone treatment for 270 min.

III.c. Diffuse Reflectance Infrared Fourier Transform Spectroscopy (DRIFTS) before and after UV−Ozone Treatment. The samples were prepared by repeatedly drop-casting a suspension of nanoparticles onto an aluminum foil and characterized with diffuse reflectance infrared Fourier transform spectroscopy (DRIFTS). Figure 4a shows infrared spectra of TTAB-coated platinum nanocubes as a function of irradiation time, revealing the rapid disappearance of the 14 carbon alkyl chain, while the quaternary ammonium moieties remain unchanged after 120 min of treatment. The spectra exhibit peaks at 3024 cm^{-1} (N^+-CH_3, C−H asym str), 2951 cm^{-1} (N^+-CH_3, C−H sym str), 960 cm^{-1} (N^+-CH_3, C−N str), 2913 cm^{-1} (CH_2, C−H asym. str.), 2863 cm^{-1} (CH_3, C−H sym str.), 2846 cm^{-1} (CH_2, C−H sym str.),1453 cm^{-1} (δ CH_2, def scissor), 1374 cm^{-1} (δ CH_3 sym. def., bend umbrella), 906 cm^{-1} (δ N^+-CH_3, C−H rocking), and 743 cm^{-1} (C_4N^+, sym. C_4N^+ skeletal mode), 507 cm^{-1} (δ C_4N^+, C_4N^+ def.).

Figure 4b shows infrared spectra of PVP-coated platinum nanocubes as a function of irradiation time. In this case, the vibrational signature in the C−H stretch region disappears completely after 59 h of treatment, and the peaks that correspond to the pyrrolidone monomers[28] take a longer time to disappear but their disappearance is not negligible. The spectra exhibit peaks at 1676 cm^{-1} (C═O, C−N str.), 1423 cm^{-1} (C−H deformation of cyclic C−H group), 1280 cm^{-1} (C−N str.),

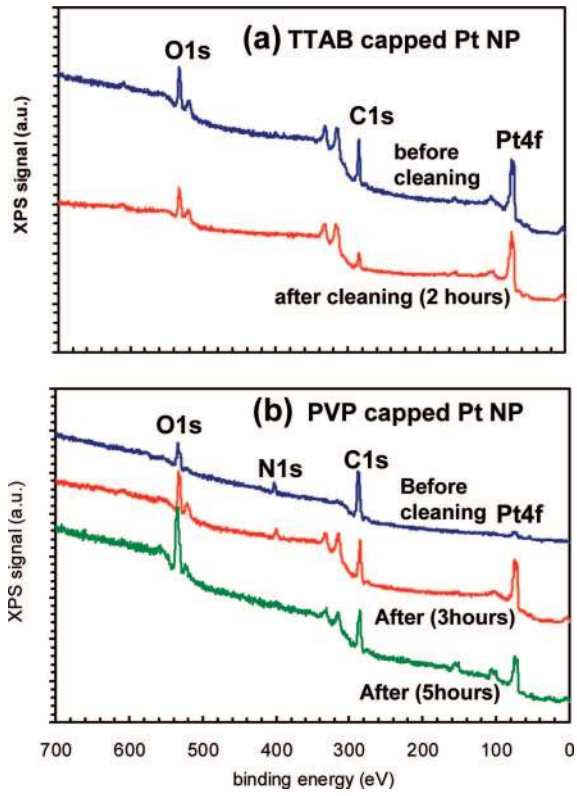

Figure 3. XPS results of (a) TTAB-coated and (b) PVP-coated Pt nanocubes deposited on a silicon wafer before and after UV−ozone treatment.

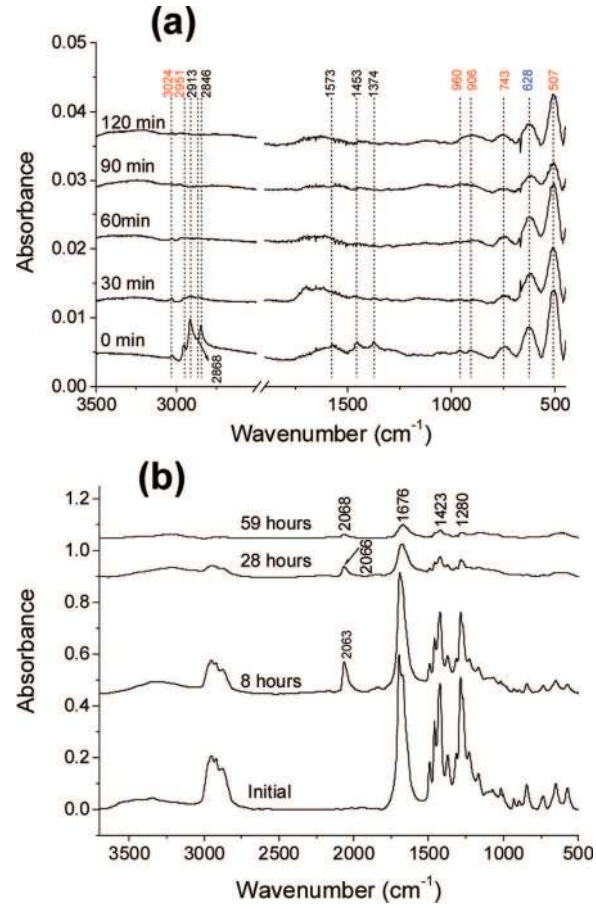

Figure 4. FTIR spectra of (a) TTAB-coated platinum nanocubes and (b) PVP-coated platinum nanocubes as a function of irradiation time.

3000−2850 cm^{-1} (C−H str.), and 2063−2068 cm^{-1} (CO str. region). However, no direct comparison of the degradation times of TTAB and PVP can be established here because there was no quantification of the number of coated nanoparticles deposited during the drop-casting procedure and the amount of nonbound capping agent, which is usually present in addition to the bound one even after a thorough washing procedure following the synthesis step. Also, the samples used in the DRIFTS experiments consist of thick, multilayered drop-cast films of nanoparticles as a result of the lower sensitivity of the technique.

III.d. Sum Frequency Generation Vibrational Spectroscopy of Pt Nanoparticles before and after UV−Ozone Treatment. Figure 5 shows SFG spectra of TTAB- and PVP-coated platinum nanoparticle arrays prepared with the Langmuir−Blodgett technique and by drop-casting, respectively, at room temperature and under vacuum (~10^{-5} Torr), at different irradiation times, and at ppp polarization. The vibrational modes of TTAB (Figure 5a) correspond to the CH_2 symmetric stretch (2850 cm^{-1}), CH_3 symmetric stretch (2875 cm^{-1}), CH_2 asymmetric stretch (2909 cm^{-1}), methyl Fermi resonance (2937 cm^{-1}), and CH_3 asymmetric stretch (2970 cm^{-1}) assigned from previous studies on TTAB with FTIR.[29] This suggests that the SFG resonance signal originates mainly from the 14 carbon alkyl chain because no vibrational contributions arising from the methylene groups directly bound to the nitrogen atom are observed. Additionally, the significant presence of methylene contributions is typical of organic adsorbates on rough surfaces, providing evidence of the disorder of the alkyl chains at the surface.[30]

The vibrational spectrum of PVP-coated nanoparticles (Figure 5b) shows the asymmetric CH_2 stretch from the ring (2960 cm^{-1}), the symmetric CH_2 stretch from the ring (2900 cm^{-1}), and the C−H stretch (2860 cm^{-1}), in agreement with previous Raman studies on PVP-capped platinum nanoparticles.[29] The UV−O_3 treatment eliminates the SFG signal after 15 min for the TTAB-coated particles and after 90 min for the PVP-coated ones.

III.e. Ethylene Hydrogenation on UV−Ozone-Treated Nanoparticles as Probed by SFGVS. The aim of removing the capping agent from the surface of the catalytic nanoparticles is to enable the study of catalytic reactions with SFGVS in the region of carbon−hydrogen stretch vibrational modes (2800−3200 cm^{-1}), which would otherwise be masked by the contribution from the capping agent's own vibrations. A reaction that has been well studied on platinum single-crystal surfaces is ethylene hydrogenation due to the molecule's structural simplicity and the few intermediates and product. It is well established that ethylene adsorbs as ethylidine and di-σ-bonded species, with π-bonded ethylene and ethyl intermediates, as probed with SFGVS on Pt (100) and Pt(111), at room temperature and 760 Torr.[31−33] The same reaction was tested with the current system at atmospheric pressure and room temperature, and the results are shown in Figure 6 for TTAB-capped Pt cubes after UV−ozone treatment. The peaks at 2878 and 2910 cm^{-1} and at 3023 cm^{-1} correspond to ethylidyne and di-σ-bonded species, respectively.

It is also worth mentioning that for the two capping agents studied, the UV−ozone treatment does not seem to remove all organic adsorbates completely as evidenced by the DRIFTS measurements. For TTAB, even though the aliphatic chains are eliminated in a relatively short time, some of the vibrational features of the hydrophilic ammonium moieties remain un-

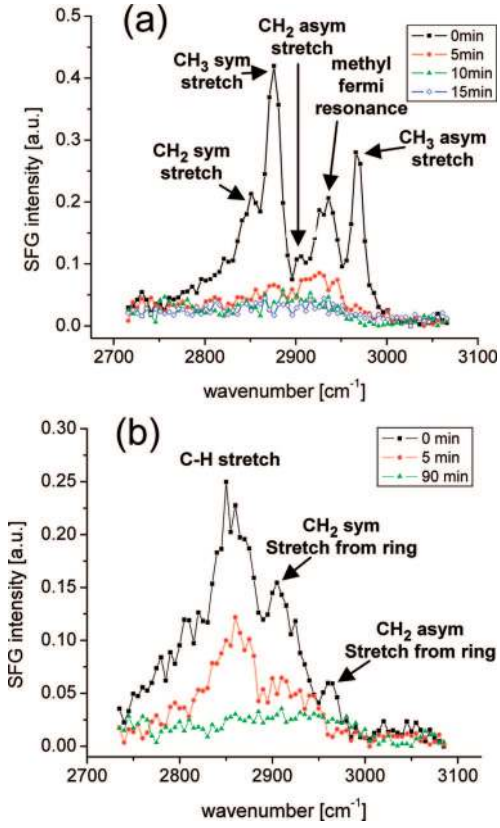

Figure 5. (a) SFGVS spectra of a Langmuir−Blodgett film of 10 nm TTAB-capped platinum cubes. The vibrational modes correspond to the CH_2 symmetric stretch (2850 cm^{-1}), CH_3 symmetric stretch (2875 cm^{-1}), CH_2 asymmetric stretch (2909 cm^{-1}), methyl Fermi resonance (2937 cm^{-1}), and CH_3 asymmetric stretch (2970 cm^{-1}). (b) SFGVS spectra of a drop-cast film of 10 nm PVP-capped platinum cubes showing a decrease in signal with irradiation time. The vibrational modes correspond to the asymmetric CH_2 stretch from the ring (2960 cm^{-1}), the symmetric CH_2 stretch from the ring (2900 cm^{-1}), and the C−H stretch (2860 cm^{-1}).

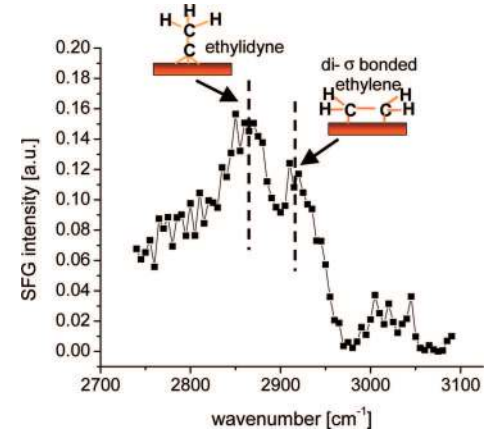

Figure 6. SFG spectra of a drop-cast film of a 10 nm TTAB-capped platinum cube under ethylene hydrogenation conditions. The spectrm shows contributions from ethylidine and di-σ-bonded ethylene adsorbates. A very small contribution from the intermediate π-bonded species is also visible at 760 Torr and 298 K.

changed even after several hours of treatment. Those moieties show carbon−nitrogen stretches characteristic of simple ammonium cations or trimethyl amine, in agreement with previous results on the thermal degradation of TTAB at the surface of platinum nanoparticles, as in the work of Borodko et al.,[34] where it is shown that the aliphatic tails are initially degraded and above 200 °C the surface remains coated with a layer of ammonium cations, which is thermally stable up to 350 °C.

For PVP, the UV−ozone treatment appears to produce pyrrolidone monomers, according to the DRIFTS analysis and similarly to previous studies on the thermal degradation of PVP on platinum nanoparticles.[28] However, the surface concentration of those monomers steadily decreases with the time of treatment, conversely to the case of thermal treatment where cross-linking of the polymer chains occurs at 200 °C, as evidenced by an increase in the intensity of the overtone of the carbonyl stretch at 3305 cm^{-1}, ultimately leading to the generation of amorphous carbon.[29] The UV−ozone approach for capping agent removal from metallic nanoparticles appears thus to be a promising alternative technique to the traditional methods.

The catalytic study conducted in this work shows many similarities with previous SFGVS studies of ethylene hydrogenation on platinum (100) and platinum (111) single crystals. That reaction has been extensively studied,[33] and it has been shown that the ratio of the di-σ-bonded peaks to the ethylidyne peaks is much smaller at the platinum (111) surface than at the platinum (100) single crystals, indicating that there is a higher concentration of ethylidyne at the surface of platinum (111).[31] In the present investigation, the ratio of di-σ-bonded to ethylidyne peak amplitudes is roughly the same compared to the platinum (100) case. This is consistent with the surface structure of the platinum nanocubes that possess the preferential face of (100).[6,35]

IV. Conclusions

UV−ozone treatment was successfully applied to the surface of platinum nanoparticles capped with TTAB and PVP, and the absence of capping layers and the preservation of the shape and spatial distribution of the nanoparticles were confirmed with SFGVS, DRIFTS, XPS, SEM, and TEM. After the removal of the capping layer, reaction intermediates of ethylene hydrogenation were identified under reaction conditions using SFGVS. The results indicate the similarity between the platinum nanoparticles and the platinum single-crystal surface. This constitutes a contribution to bridging the materials gap from single crystals to nanoparticle systems and allows for future SFGVS studies of catalytic reactions on reasonably clean metallic nanoparticles. However, even though UV−ozone cleaning constitutes a useful tool in the spectroscopic study of catalytic reactions on metals, from a catalysis standpoint its effects are still not fully understood and are currently under investigation.

Note Added after ASAP Publication. This article was published ASAP on February 20, 2009. The caption to Figure 6 has been modified. The correct version was published on March 6, 2009.

Acknowledgment. This work was supported by the Director, Office of Science, Office of Basic Energy Sciences, Division of Chemical Sciences, Geological and Biosciences and Division of Materials Sciences and Engineering of the U.S. Department of Energy under contract no. DE-AC02-05CH11231. H.S.L gratefully acknowledges financial aid from the Korea Research Foundation Grant funded by the Korean Government.

References and Notes

(1) Somorjai, G., A.; Park, J. Y. *Catal. Lett.* **2007**, *115*, 87.
(2) Bell, A. T. *Science* **2003**, *299*, 1688.
(3) Unterhalt, H.; Rupprechter, G.; Freund, H.-J. *J. Phys. Chem. B* **2002**, *106*, 356.
(4) Somorjai, G. A.; Park, J. Y. *Phys. Today* **2007**, *60*, 48.

(5) Park, J. Y.; Zhang, Y.; Grass, M.; Zhang, T.; Somorjai, G. A. *Nano Lett.* **2008**, *8*, 673.
(6) Lee, H.; Habas, S. E.; Kweskin, S. J.; Butcher, D.; Somorjai, G. A.; Yang, P. *Angew. Chem.* **2006**, *45*, 7824.
(7) Humphrey, S. M.; Grass, M. E.; Habas, S. E.; Niesz, K.; Somorjai, G. A.; Tilley, T. D. *Nano Lett.* **2007**, *7*, 785.
(8) Bartholomew, C. H.; Agrawal, P. K.; Katzer, J. R. *Adv. Catal.* **1982**, *31*, 135.
(9) Park, J. Y.; Lee, H.; Renzas, J. R.; Zhang, Y. W.; Somorjai, G. A. *Nano Lett.* **2008**, *8*, 2388.
(10) Kweskin, S. J.; Rioux, R. M.; Habas, S. E.; Komvopoulos, K.; Yang, P.; Somorjai, G. A. *J. Phys. Chem. B* **2006**, *110*, 15920.
(11) Grunes, J.; Zhu, J.; Yang, M.; Somorjai, G. A. *Catal. Lett.* **2003**, *86*, 157.
(12) Waldrup, S. B.; Williams, C. T. *Catal. Commun.* **2007**, *8*, 1373.
(13) Bratlie, K. M.; Komvopoulos, K.; Somorjai, G. A. *J. Phys. Chem. C* **2008**, *112*, 11865.
(14) Zaera, F.; Somorjai, G. A. *J. Am. Chem. Soc.* **1984**, *106*, 2288.
(15) Kliewer, C. J.; Bieri, M.; Somorjai, G. A. *J. Phys. Chem. C* **2008**, *112*, 11373.
(16) Vig, J. R. *J. Vac. Sci. Technol., A* **1985**, *3*, 1027.
(17) Ye, H. K.; Gu, Z. Y.; Gracias, D. H. *Langmuir* **2006**, *22*, 1863.
(18) Zhang, D.; Dougal, S. M.; Yeganeh, M. S. *Langmuir* **2000**, *16*, 4528.
(19) Stokes, G. Y.; Buchbinder, A. M.; Gibbs-Davis, J. M.; Scheidt, K. A.; Geiger, F. M. *J. Phys. Chem. A* **2008**, *112*, 11688.
(20) Pang, S.; Kurosawa, Y.; Kondo, T.; Kawaii, T. *Chem. Lett.* **2005**, *34*, 544.
(21) Chen, W.; Kim, J.; Sun, S.; Chen, S. *Phys. Chem. Chem. Phys.* **2006**, *8*, 2779.
(22) Zhang, Y.; Grass, M. E.; Habas, S. E.; Tao, F.; Zhang, T.; Yang, P.; Somorjai, G. A. *J. Phys. Chem. C* **2007**, *111*, 12243.
(23) Yeganeh, M. S.; Dougal, S. M.; Silbernagel, B. G. *Langmuir* **2006**, *22*, 637.
(24) Srivastava, A.; Eisenthal, K. *Chem. Phys. Lett.* **1998**, *292*, 345.
(25) Shen, Y. R. *The Principles of Nonlinear Optics*; John Wiley and Sons: New York, 1984.
(26) Buck, M.; Himmelhaus, M. *J. Vac. Sci. Technol., A* **2001**, *19*, 2717.
(27) Bloembergen, N. *Nonlinear Optics*; W. A. Benjamin: New York, 1965.
(28) Borodko, Y.; Humphrey, S. M.; Tilley, T. D.; Frei, H.; Somorjai, G. A. *J. Phys. Chem. C* **2007**, *111*, 6288.
(29) Borodko, Y.; Habas, S. E.; Koebel, M.; Yang, P.; Frei, H.; Somorjai, G. A. *J. Phys. Chem. B* **2006**, *110*, 23052.
(30) Bordenyuk, A., N.; Weeraman, C.; Yatawara, A., K.; Jayathilake, H. D.; Stiopkin, I.; Liu, Y.; Benderskii, A. V. *J. Phys. Chem. C* **2007**, *111*, 8925.
(31) Somorjai, G. A.; McCrea, K. R.; Zhu, J. *Top. Catal.* **2002**, *18*, 157.
(32) Cremer, P. S.; Su, X.; Shen, Y.-R.; Somorjai, G. A. *J. Am. Chem. Soc.* **1996**, *118*, 2942.
(33) Sheppard, N.; DelaCruz, C. In *Vibrational Spectra of Hydrocarbons Adsorbed on Metals 0.1. Introductory Principles, Ethylene, and the Higher Acyclic Alkenes*; Advances in Catalysis; Academic Press: San Diego, 1996; Vol. 41, p 1.
(34) Borodko, Y.; Jone, L.; Lee, H.; Yang, P.; Frei, H.; Somorjai, G. A. 2008, submitted for publication.
(35) Habas, S. E.; Hyunjoo, L.; Radmilovic, V.; Somorjai, G. A. *Nat. Mater.* **2007**, *6*, 692.

JP8108946